

Reevaluation of the transition-moment function and Einstein coefficients for the $N_2(A\ ^3\Sigma_u^+ - X\ ^1\Sigma_g^+)$ transition

Lawrence G. Piper

Physical Sciences Inc., Andover, Massachusetts 01810

(Received 4 December 1992; accepted 28 April 1993)

We have measured the relative intensities of the nitrogen Vegard–Kaplan bands $N_2(A\ ^3\Sigma_u^+ - X\ ^1\Sigma_g^+)$ for transitions covering a range in r centroids between 1.22 and 1.48 Å. With this data we constructed a relative electronic transition moment function that diverges significantly from previously reported functions. We place our data on an absolute basis by normalizing our relative function by the experimentally determined Einstein coefficient for the $v'=0$ to $v''=6$ transition. Combining our normalized data from 1.22 to 1.48 Å with absolute transition moment data measured by Shemansky between 1.08 and 1.14 Å results in a function covering the range between 1.08 and 1.48 Å. The radiative lifetimes calculated from this function are longer than those currently accepted by amounts varying between 25% for $v'=0$ –50% for $v'=4$ –6.

I. INTRODUCTION

For most of the last 20 years, the radiative lifetime of $N_2(A\ ^3\Sigma_u^+)$ has been accepted to be 1.9 s. This lifetime and the associated Einstein coefficients for $N_2(A\ ^3\Sigma_u^+ - X\ ^1\Sigma_g^+)$ transitions, the Vegard–Kaplan bands, are based on Shemansky's¹ measurements of the absorption coefficients of the 6–0 through 12–0 Vegard–Kaplan bands in the vacuum ultraviolet and his reanalysis² of a measurement by Carleton and Oldenberg³ of the Einstein coefficient of the 0–6 transition.

Carleton and Oldenberg³ simultaneously measured the absolute photon-emission rate of the 0–6 Vegard–Kaplan band and the absolute number density in $v'=0$ of the A state via resonance absorption on the 1–0 transition of the nitrogen first-positive system $N_2(B\ ^3\Pi_g - A\ ^3\Sigma_u^+)$. Shemansky and Carleton² corrected the original data with an improved set of line strength factors needed to analyze the absorption measurements correctly. Assuming that the experimental observations of Carleton and Oldenberg are accurate, and that the reanalysis of the absorption measurements is correct, then the derived Einstein coefficient for the 0,6 Vegard–Kaplan band depends directly on the accuracy of the Einstein coefficient for the 1,0 band of the first-positive system. Shemansky and Carleton used the value of $8.48 \times 10^4\ s^{-1}$ calculated by Shemansky and Vallance Jones⁴ using the Franck–Condon factors of Benesch *et al.*⁵ and Jeunehomme's⁶ transition-moment function.

Several years ago, we questioned the accuracy of some of the input data used to analyze the Carleton and Oldenberg experiment⁷ and suggested that the radiative lifetime of $N_2(A, v=0)$ could be 40% larger than the accepted value. Werner *et al.*⁸ *ab initio* calculations of the electronic transition moment for the $N_2(B\ ^3\Pi_g - A\ ^3\Sigma_u^+)$ transition appeared to support our contention. Their results indicated the accepted values for the radiative lifetimes of the lowest vibrational levels of $N_2(B)$ were probably seriously in error, perhaps being as much as 40% too low. This suggested to us that the Einstein coefficient for the $N_2(B-A)$ 1,0 transition could be in error by a like amount. The result then would be a 40% error in the $N_2(A)$ lifetime

derived from the Carleton and Oldenberg experiment.

Our subsequent experimental determination⁹ of the $N_2(B-A)$ transition-moment variation confirmed Werner *et al.* set of theoretically calculated lifetimes. The corrected value of the 1,0 Einstein coefficient of the N_2 first-positive system $7.48 \times 10^4\ s^{-1}$, however, is only 12% less than that of Shemansky and Vallance Jones. This reasonable agreement between the two Einstein coefficients is fortuitous because the two transition-moment functions happen to be close together at the internuclear separation appropriate to the 1,0 transition. They diverge widely at other internuclear separations and give much different Einstein coefficients for other important transitions.

The uncertainty in the data used to derive the Einstein coefficients for the Vegard–Kaplan bands is stated¹ to be about 20%. Making a 12% correction to these Einstein coefficients, therefore, hardly seems justified. However, our difficulties fitting Vegard–Kaplan spectra, particularly at wavelengths larger than 400 nm, indicated that the shape of the transition-moment function might be errant. A re-investigation therefore seemed warranted.

We have measured relative intensities in a number of Vegard–Kaplan bands covering a range of wavelengths between 220 and 500 nm. The transition moment function we derive from these data differs significantly from those previously proposed.^{10–12} Einstein coefficients calculated with our transition-moment function are up to 60% smaller than those Shemansky published and our calculated radiative lifetimes are between 25% and 60% longer for $v'=0$ –6.

II. EXPERIMENT

The experimental apparatus (see Fig. 1) is a 2 in. diameter discharge-flow reactor configured to allow spectral observations along the flow tube axis. $N_2(A)$ entered the observation vessel from a sidearm normal to the flow tube axis, but parallel with and just in front of the slits of the monochromator used for the spectral measurements. A CaF_2 window sealed the upstream end of the flow tube. The window transmission is nearly uniform over the spec-

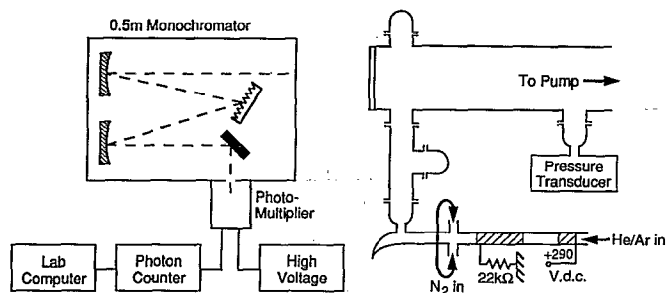


FIG. 1. Discharge-flow reactor for observing $N_2(A^3\Sigma_u^+ - X^1\Sigma_g^+)$ emission.

tral range investigated in these studies 220–500 nm. Small reductions in transmission at the shortest wavelengths were incorporated into the data analysis.

The energy transfer reaction between metastable $Ar^*(^3P_{0,2})$ and N_2 (Refs. 13 and 14) generated $N_2(A)$. This reaction produces $N_2(C^3\Pi_u)$ which radiates immediately to the $N_2(B^3\Pi_g)$ state. Subsequent radiative and collisional cascade from $N_2(B)$ makes the highly metastable $N_2(A^3\Sigma_u^+)$. A low-power, hollow-cathode discharge, sustained in a flow of argon or 5%–10% argon in helium produced Ar^* . N_2 mixed with Ar^* downstream from the discharge. Helium bath gas relaxes the vibrational distribution of $N_2(A)$ so that only $v' \leq 2$ is observed (see Fig. 2). In an argon bath gas, emission from $v' \leq 4$ is readily observed (see Fig. 3).

A 0.5 m monochromator having a 1200 line mm^{-1} grating blazed at 250 nm collected and dispersed radiation emanating from the flow tube. A thermoelectrically cooled HTV R943-02 photomultiplier tube connected to a photon-counting rate meter and lab computer detected the dispersed radiation.

The relative variation in monochromator response as a function of wavelength was determined from measurements of the spectra emitted from standard D_2 (180–400 nm) and quartz-halogen lamps (280–500 nm) (Optronic

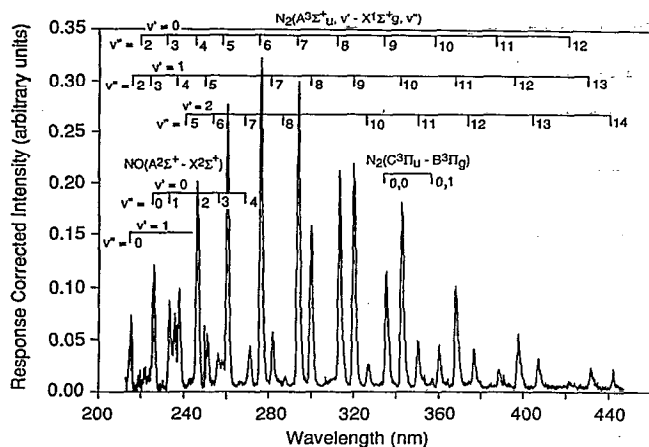


FIG. 2. Emission between 215 and 450 nm from $N_2(A)$ in helium. Note that the 0,1 band of the $N_2(C-B)$ system is barely visible at 358 nm.

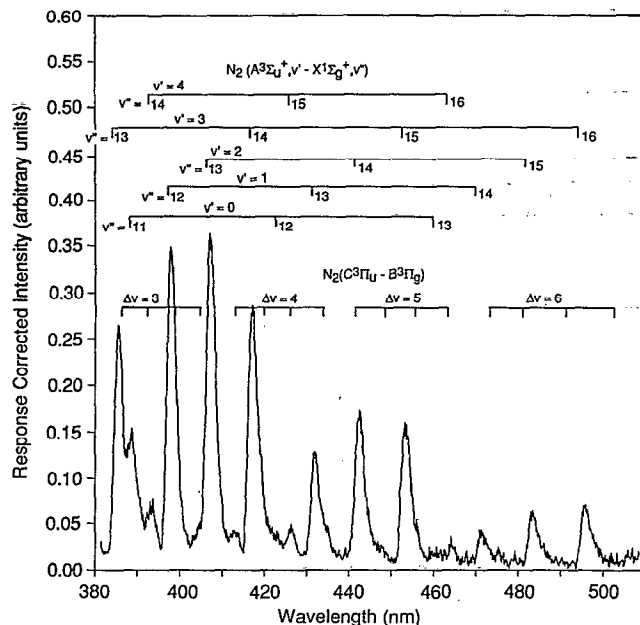


FIG. 3. Emission between 380 and 500 nm from $N_2(A)$ in argon.

Laboratories). The lamp output was reflected into the monochromator off a uniformly scattering, diffuse white target (Spectralon). This procedure ensured that the monochromator optics were filled and eliminated possible errors resulting from such things as nonuniformities in reflectivity across the face of the grating or in sensitivity across the face of the photomultiplier. The two lamps gave congruent response functions (within 5%) over the spectral region common to them both, 280–400 nm.

Most of the spectra were generated at conditions that minimized, as much as possible, interfering emissions from the nitrogen second-positive bands $N_2(C^3\Pi_u - B^3\Pi_g)$ and the NO gamma bands $NO(A^2\Sigma^+ - X^2\Pi)$. $N_2(A)$ energy pooling reactions generate the second-positive emission¹⁵ while the energy transfer reaction between $N_2(A)$ and NO excites the gamma bands.⁷ The hollow cathode discharge makes small number densities of NO from the impurities in the gases used. The advantage of the axial observation configuration is that band intensity measurements with good signal to noise ratio can be made with $N_2(A)$ number densities sufficiently low that $N_2(C^3\Pi_u)$ production from $N_2(A)$ energy pooling is relatively minor, and at total pressures low enough to keep NO production rates in the d.c. discharge small.

A spectral fitting procedure we have detailed previously⁹ aided data analysis. Synthetic spectra are generated by first multiplying a set of vibronic level populations by a set of basis functions representing the intensity of a unit population of each vibronic level as a function of wavelength. The intensities of each band at each wavelength increment are then summed to determine an overall spectral intensity. A least squares solution determines the set of vibronic level populations giving a predicted spectrum that best matches the experimental one. The important spectral features between 200 and 500 nm are the nitrogen Vegard-

Kaplan bands $N_2(A^3\Sigma_u^+ - X^1\Sigma_g^+)$, nitrogen second-positive bands $N_2(C^3\Pi_u - B^3\Pi_g)$, and nitric oxide gamma bands $NO(A^2\Sigma^+ - X^2\Pi)$.

To generate synthetic spectra, we used the spectroscopic constants of Roux *et al.*^{16,17} for the A and B electronic states of N_2 , those in Lofthus and Krupenie¹⁸ for the C and X states of N_2 , and those tabulated in Huber and Herzberg¹⁹ for NO A and X . Einstein coefficients used in the fit were from Lofthus and Krupenie for $N_2(C-B)$ (Ref. 18) and Piper and Cowles for $NO(A-X)$.²⁰ We calculated a set of Franck-Condon factors and r centroids for $N_2(A-X)$ using procedures we have outlined previously.²¹ These Franck-Condon factors are quite similar to those calculated by Benesch *et al.*⁵ which are tabulated in Lofthus and Krupenie.¹⁸

III. TRANSITION MOMENT VARIATIONS

Our data analysis is based on the r -centroid approximation as first described by Fraser²² and developed by Nicholls²³ and McCallum.²⁴ The intensity of radiative emission from an electronic transition is given by the product of the upper state number density and the Einstein coefficient for spontaneous radiation

$$I_{v'v''} = N_{v'} A_{v'v''} \quad (1)$$

The Einstein coefficient $A_{v'v''}$ can be written as

$$A_{v'v''} = \frac{64\pi^4}{3h} q_{v'v''} \nu_{v'v''}^3 |R_e(\bar{r}_{v'v''})|^2, \quad (2)$$

where $q_{v'v''}$ is the Franck-Condon factor for the transition; $\nu_{v'v''}$ is the transition frequency in cm^{-1} ; $R_e(\bar{r})$ is the electronic transition moment, a function of internuclear separation; and $\bar{r}_{v'v''}$ is the r centroid of the transition, an average internuclear separation for the transition. Determining Einstein coefficients requires that the variation in the transition moment as a function of internuclear separation be established over the range of important transitions and that the absolute value of the transition moment be determined for at least one point.

Relative variations in the transition moment function usually can be determined over a wide range of internuclear separations from measurements of relative band intensities in a progression from a common upper level. Dividing the measured band intensities by $q_{v'v''} \nu_{v'v''}^3$ results in reduced intensities that are a function only of the square of the transition moment

$$\frac{I_{v'v''}}{q_{v'v''} \nu_{v'v''}^3} = \kappa N_{v'} |R_e(\bar{r}_{v'v''})|^2, \quad (3)$$

where $\kappa = 64\pi^4/3h$. The form of the transition moment function is then given by a fit of the square roots of the reduced intensities to their corresponding r centroids which are, in essence, effective internuclear separations at which each transition occurs.

The relative function often can be normalized so that the sum of Einstein coefficients in a progression yield the reciprocal of the radiative lifetime of the state under investigation. In the present case, no accurate lifetime measure-

ments of the A state of nitrogen exist. What is available is Carleton and Oldenberg's³ determination of the Einstein coefficient of the 0,6 band of $N_2(A)$ as reanalyzed by Shemansky and Carleton² and corrected here for the improved value of the $N_2(B-A)$ Einstein coefficient.

Another method for obtaining absolute transition moment values is from oscillator strengths determined from absorption measurements. The transition moment in this case is given by

$$R_e(\bar{r}_{v'v''}) = \left(\frac{f_{v'v''}}{1.5\kappa q_{v'v''} \nu_{v'v''}} \right)^{1/2}. \quad (4)$$

Shemansky measured a set of oscillator strengths for the absorptions from $v''=0$ of the X state to $v'=5-12$ of the A state. These values can be converted to transition moments over the range of internuclear separations between 1.084 and 1.129 Å.

Our measurements of relative intensities of bands in four different progressions of the Vegard-Kaplan band system establish the shape of the transition moment function. Shemansky and Carleton's Einstein coefficient for the 0,6 band normalizes our data to give an absolute transition moment function for internuclear separations between 1.22 and 1.48 Å. Finally, combining our normalized data with the results of Shemansky's absorption measurements results in a transition moment function covering the range of internuclear separations between 1.08 and 1.48 Å.

IV. RESULTS

We fit our spectra in a number of segments each containing no more than one Vegard-Kaplan emission band from each of the progressions emanating from $v'=0-3$. Figures 2 and 3 show two of the spectra we took for this study, while Figs. 4 and 5 show small spectral segments to illustrate the fitting procedure. The spectral fits give relative intensities within each progression. Dividing these relative intensities by the product $q_{v'v''} \nu_{v'v''}^3$ converted them to a set of reduced intensities covering a range of wavelengths, or equivalently, r centroid values. The square root of the reduced intensities vary from one another with changes in r centroid in the same fashion that the transition moment function varies as a function of internuclear separation. Our data set consisted of the transitions $v'=0$ to $v''=2-13$; $v'=1$ to $v''=4,5,7-14$; $v'=2$ to $v''=6-8, 10-15$; and $v'=3$ to $v''=13-16$.

Our data fitting procedure involved fitting the data from just one of the progressions first. A quadratic function represented the data adequately. The other progressions were then normalized by the factor that resulted in the smallest sum of the squares of the relative residuals between the data and the initial quadratic function. The relative residual is

$$\chi = \frac{|R_e|_{\text{fit}} - |R_e|_{\text{measured}}}{|R_e|_{\text{fit}}} \quad (5)$$

We then refit this combined data set to a new quadratic function and then renormalized the reduced intensities in each progression to minimize again the sum of squares of

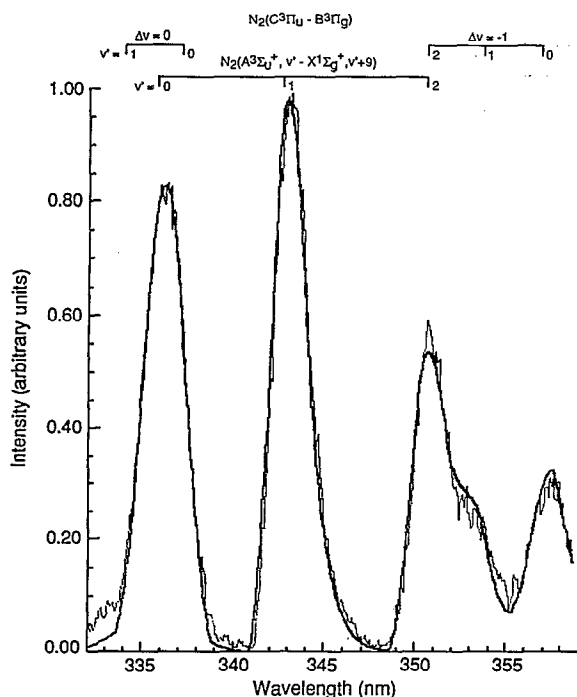


FIG. 4. $N_2(A^3\Sigma_u^+ - X^1\Sigma_g^+, \Delta v = -9)$ sequence in argon carrier. The contribution of the $N_2(C^3\Pi_u, v' = 0 - B^3\Pi_g, v'' = 0)$ band to the $N_2(A, v = 0 - X, v'' = 9)$ band at 337 nm can be removed in the spectral fitting analysis by including the $N_2(C, v' = 0 - B, v'' = 1)$ band at 357 nm in the spectral fit. The light line represents the data and the heavy line the spectral fit.

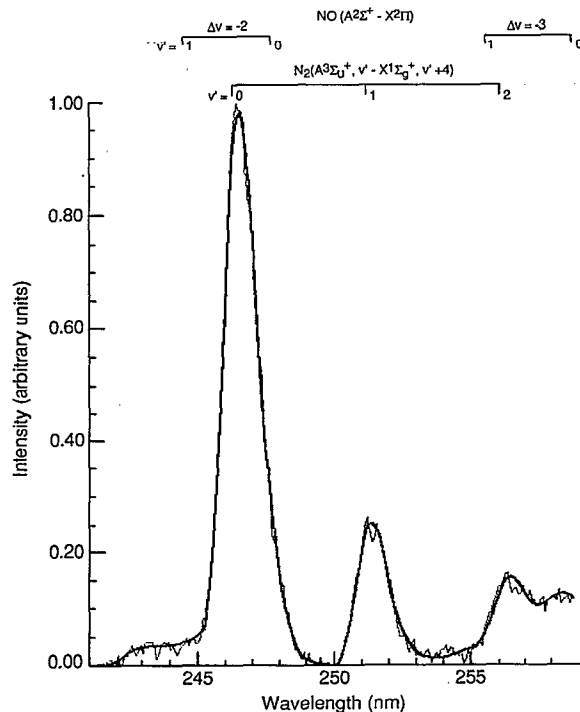


FIG. 5. $N_2(A^3\Sigma_u^+, v - X^1\Sigma_g^+, \Delta v = -4)$ sequence in helium. Extending the fit to 259 nm includes enough of the $NO(A^2\Sigma^+, v' = 0 - X^2\Pi^+, v'' = 3)$ band to allow an accurate assessment of the contribution of the $NO(A, v' = 0 - X, v'' = 2)$ band to the emission at 246 nm which is primarily the $N_2(A, v' = 0 - X, v'' = 4)$ band.

the residuals between the renormalized data and the new quadratic function. After several iterations, the renormalization procedure failed to improve the sum of squares of the residuals to any significant extent.

We then established absolute values for our relative data by multiplying each point by the factor necessary to make the value of the relative transition moment function at 1.294 Å, the r centroid for the 0,6 transition, equal to the value determined in Shemansky's reanalysis of Carleton and Oldenberg's measurement of the 0,6 Einstein coefficient, i.e., 0.0901 s^{-1} . This value has been corrected for the updated value of the $N_2(B, v' = 1 - A, v'' = 0)$ transition probability. Finally, combining our absolute values with absolute transition moment values calculated from Shemansky's oscillator strength measurements determined the transition moment function between 1.084 and 1.476 Å.

Figure 6 shows the fit of these two sets of transition moment values. The data quite nicely fit the function

$$R_e(r) = 0.00443 - 0.00582r + 0.00175r^2, \quad (6)$$

where R_e is in units of Debye and r is in Angstroms. Table I lists the Einstein coefficients calculated from the transition moment function represented by Eq. (6). Table I also lists the other spectroscopic properties—Franck-Condon factors, r centroids, and band origins.

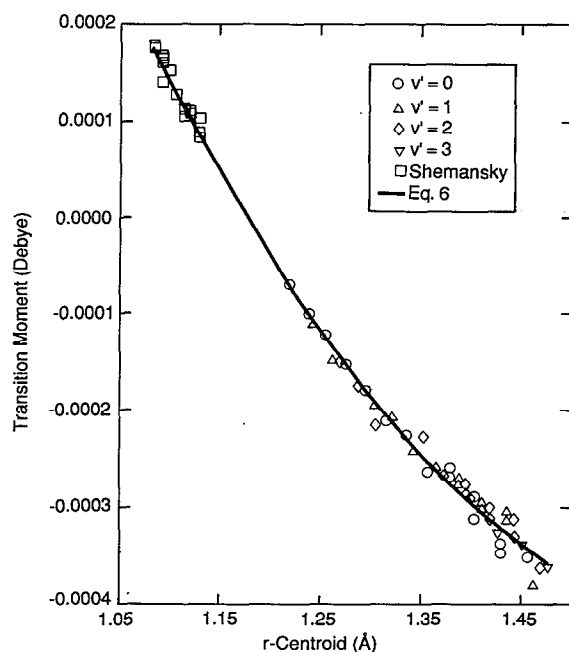


FIG. 6. Electronic transition moment data and the associated quadratic least squares fit [Shemansky (Ref. 1)].

TABLE I. $N_2(A^3\Sigma_u^+ - X^1\Sigma_g^+)$ Einstein coefficients.

v'	v''	Wave-length (nm)	$q_{v',v''}$	r centroid (Å)	Branching ratio	$A_{v',v''}$ (s^{-1})
0	0	200.99	0.000 97	1.185	0.000 02	0.000 008
	1	210.86	0.008 00	1.202	0.001 18	0.000 499
	2	221.61	0.031 94	1.219	0.010 77	0.004 544
	3	233.37	0.079 16	1.237	0.044 31	0.018 705
	4	246.26	0.139 70	1.255	0.107 40	0.045 332
	5	260.47	0.184 50	1.274	0.176 88	0.074 662
	6	276.20	0.190 50	1.294	0.212 22	0.089 579
	7	293.70	0.157 30	1.314	0.190 26	0.080 308
	8	313.28	0.106 40	1.335	0.133 87	0.056 506
	9	335.34	0.059 19	1.356	0.073 91	0.031 197
	10	360.36	0.027 42	1.379	0.033 11	0.013 976
	11	388.97	0.010 50	1.402	0.011 77	0.004 968
	12	422.00	0.003 30	1.428	0.003 36	0.001 419
	13	460.54	0.000 87	1.455	0.000 77	0.000 327
	14	506.07	0.000 20	1.479	0.000 15	0.000 063
	15	560.66	0.000 04	1.499	0.000 02	0.000 010
	16	627.30	0.000 01	1.533	0.000 00	0.000 001
		Sum=1.000 00				Lifetime=2.37 s
1	0	195.36	0.005 18	1.175	0.000 00	0.000 002
	1	204.68	0.031 85	1.191	0.001 94	0.000 734
	2	214.79	0.087 25	1.208	0.020 42	0.007 714
	3	225.81	0.131 20	1.225	0.059 93	0.022 636
	4	237.87	0.111 60	1.242	0.076 36	0.028 844
	5	251.10	0.040 87	1.260	0.037 04	0.013 991
	6	265.68	0.000 03	1.281	0.000 04	0.000 014
	7	281.84	0.036 47	1.303	0.048 48	0.018 311
	8	299.82	0.109 80	1.322	0.153 20	0.057 869
	9	319.96	0.150 10	1.342	0.212 26	0.080 179
	10	342.66	0.134 70	1.364	0.188 35	0.071 145
	11	368.44	0.088 84	1.387	0.118 70	0.044 839
	12	397.94	0.045 35	1.410	0.055 67	0.021 030
	13	432.03	0.018 46	1.435	0.020 27	0.007 657
	14	471.85	0.006 10	1.461	0.005 78	0.002 185
	15	518.97	0.001 67	1.487	0.001 31	0.000 497
	16	575.56	0.000 38	1.513	0.000 24	0.000 090
		Sum=0.999 85				Lifetime=2.65 s
2	0	190.14	0.014 76	1.164	0.000 86	0.000 298
	1	198.95	0.065 13	1.180	0.000 33	0.000 114
	2	208.50	0.113 30	1.197	0.013 85	0.004 807
	3	218.87	0.082 21	1.213	0.026 21	0.009 097
	4	230.17	0.011 24	1.227	0.005 69	0.001 976
	5	242.54	0.014 83	1.254	0.014 18	0.004 921
	6	256.12	0.077 37	1.269	0.086 41	0.029 990
	7	271.10	0.081 23	1.287	0.104 65	0.036 319
	8	287.70	0.021 88	1.304	0.030 16	0.010 466
	9	306.20	0.003 70	1.340	0.006 38	0.002 213
	10	326.92	0.062 30	1.352	0.098 59	0.034 218
	11	350.30	0.127 80	1.372	0.193 91	0.067 299
	12	376.86	0.138 00	1.394	0.196 55	0.068 217
	13	407.30	0.100 50	1.418	0.131 09	0.045 498
	14	442.51	0.053 90	1.442	0.062 01	0.021 522
	15	483.69	0.022 29	1.468	0.021 97	0.007 627
	16	532.49	0.007 28	1.495	0.005 93	0.002 058
	17	591.20	0.001 91	1.524	0.001 23	0.000 428
		Sum=0.999 63				Lifetime=2.88 s
3	0	185.29	0.030 14	1.155	0.006 30	0.002 032
	1	193.65	0.093 36	1.170	0.001 39	0.000 450
	2	202.68	0.091 09	1.186	0.002 99	0.000 963
	3	212.46	0.015 29	1.200	0.002 47	0.000 797
	4	223.10	0.015 21	1.224	0.008 11	0.002 617
	5	234.70	0.072 27	1.239	0.055 27	0.017 831
	6	247.39	0.045 87	1.255	0.045 50	0.014 682
	7	261.34	0.000 04	1.276	0.000 06	0.000 018

TABLE I. (Continued.)

v'	v''	Wave-length (nm)	$q_{v',v''}$	r centroid (Å)	Branching ratio	$A_{v',v''}$ (s^{-1})
	8	276.73	0.042 17	1.297	0.063 81	0.020 587
	9	293.80	0.080 66	1.314	0.127 50	0.041 135
	10	312.83	0.036 47	1.332	0.058 46	0.018 861
	11	334.17	0.000 12	1.357	0.000 19	0.000 062
	12	358.26	0.046 25	1.382	0.075 98	0.024 514
	13	385.66	0.116 60	1.403	0.176 51	0.056 950
	14	417.09	0.134 20	1.426	0.183 12	0.059 081
	15	453.48	0.098 84	1.450	0.117 92	0.038 045
	16	496.10	0.052 19	1.476	0.052 90	0.017 066
	17	546.68	0.020 85	1.503	0.017 31	0.005 584
	18	607.65	0.006 47	1.532	0.004 23	0.001 365
		Sum=0.998 09				Lifetime=3.10 s
4	0	180.77	0.048 55	1.146	0.023 65	0.007 298
	1	188.71	0.099 80	1.161	0.010 45	0.003 226
	2	197.28	0.041 69	1.176	0.000 00	0.000 000
	3	206.54	0.002 79	1.201	0.000 56	0.000 171
	4	216.58	0.058 74	1.211	0.019 52	0.006 026
	5	227.49	0.041 21	1.226	0.023 41	0.007 226
	6	239.40	0.000 37	1.246	0.000 34	0.000 104
	7	252.44	0.048 71	1.265	0.059 03	0.018 220
	8	266.77	0.053 12	1.281	0.073 26	0.022 610
	9	282.60	0.002 30	1.303	0.003 72	0.001 147
	10	300.16	0.030 80	1.325	0.054 20	0.016 729
	11	319.75	0.076 34	1.342	0.132 38	0.040 859
	12	341.74	0.037 68	1.361	0.063 42	0.019 575
	13	366.58	0.000 08	1.387	0.000 13	0.000 039
	14	394.86	0.047 13	1.413	0.073 76	0.022 764
	15	427.33	0.117 70	1.434	0.162 64	0.050 199
	16	464.97	0.131 50	1.458	0.157 53	0.048 620
	17	509.12	0.092 46	1.484	0.093 31	0.028 799
	18	561.59	0.045 96	1.512	0.037 78	0.011 660
	19	624.95	0.017 03	1.540	0.010 91	0.003 367
		Sum=0.993 96				Lifetime=3.24 s
5	0	176.55	0.067 26	1.137	0.062 28	0.018 734
	1	184.12	0.085 52	1.152	0.026 51	0.007 974
	2	192.27	0.006 54	1.163	0.000 49	0.000 148
	3	201.05	0.032 50	1.185	0.001 01	0.000 304
	4	210.55	0.053 13	1.199	0.009 00	0.002 707
	5	220.85	0.000 95	1.215	0.000 38	0.000 113
	6	232.06	0.038 26	1.236	0.029 63	0.008 914
	7	244.29	0.045 01	1.251	0.045 11	0.013 570
	8	257.68	0.000 12	1.270	0.000 16	0.000 048
	9	272.42	0.040 74	1.291	0.063 57	0.019 122
	10	288.71	0.050 86	1.307	0.083 57	0.025 139
	11	306.79	0.002 10	1.311	0.003 02	0.000 909
	12	326.97	0.031 81	1.353	0.058 62	0.017 634
	13	349.64	0.073 47	1.371	0.128 15	0.038 550
	14	375.27	0.030 25	1.389	0.048 76	0.014 667
	15	404.48	0.001 50	1.442	0.002 61	0.000 785
	16	438.05	0.059 04	1.443	0.081 28	0.024 451
	17	477.02	0.124 40	1.467	0.147 11	0.044 252
	18	522.79	0.125 10	1.493	0.123 28	0.037 086
	19	577.27	0.079 99	1.520	0.063 50	0.019 102
	20	644.63	0.035 98	1.549	0.021 97	0.006 609
		Sum=0.984 54				Lifetime=3.32 s
6	0	172.61	0.082 11	1.128	0.121 91	0.036 835
	1	179.84	0.057 88	1.143	0.036 69	0.011 085
	2	187.60	0.001 56	1.168	0.000 05	0.000 015
	3	195.96	0.054 52	1.175	0.000 03	0.000 010
	4	204.97	0.016 26	1.187	0.000 72	0.000 216
	5	214.72	0.016 72	1.210	0.005 63	0.001 702
	6	225.29	0.048 19	1.224	0.026 12	0.007 892
	7	236.80	0.001 94	1.228	0.001 09	0.000 328

TABLE I. (Continued.)

v'	v''	Wave-length (nm)	$q_{v'v''}$	r centroid (Å)	Branching ratio	$A_{v'v''}$ (s^{-1})
8		249.37	0.033 07	1.261	0.039 16	0.011 833
9		263.15	0.040 04	1.276	0.053 71	0.016 230
10		278.31	0.000 00	1.297	0.000 01	0.000 002
11		295.08	0.042 63	1.318	0.074 41	0.022 482
12		313.70	0.043 60	1.334	0.075 63	0.022 851
13		334.51	0.000 17	1.358	0.000 31	0.000 094
14		357.90	0.041 00	1.382	0.071 88	0.021 720
15		384.37	0.069 43	1.400	0.111 34	0.033 641
16		414.56	0.017 80	1.417	0.025 21	0.007 617
17		459.30	0.008 43	1.461	0.011 57	0.003 495
18		489.67	0.079 97	1.477	0.090 34	0.027 296
19		537.16	0.132 50	1.502	0.123 30	0.037 255
20		594.97	0.114 40	1.529	0.084 48	0.025 526
21		664.60	0.063 93	1.558	0.036 09	0.010 906
22		751.24	0.025 13	1.589	0.010 33	0.003 120
			Sum=0.849 73			
				Lifetime=3.31 s		

V. DISCUSSION

A. Relative transition moment function comparison

Three other groups have reported relative transition moment functions based on measurements of relative Vegard–Kaplan band intensities.^{10–12} We have reanalyzed all three sets of relative intensity measurements because our RKR-based (Rydberg–Klein–Rees) Franck–Condon factors are substantially different from the Franck–Condon factors used by Carleton and Papioliolis¹⁰ and Chandraiah and Shepherd.¹¹ Broadfoot and Maran¹² do not list the Franck–Condon factors they used in their analysis, but since they came from the widely disseminated, albeit unpublished compendium of Albritton *et al.*,²⁵ they are most likely quite similar to the ones we have calculated.

We find that all three sets of band intensity measurements give relative transition moment values that are consistent with each other. However, they are not at all consistent with our measurements nor, for that matter, with Shemansky's transition moment function. Figure 7 compares the data from these three earlier sets of measurements, normalized to each other at 1.294 Å, to Shemansky's quadratic function and to our functional fit from Eq. (6). The previous measurements all show a slight, but clearly identifiable convex curvature, whereas Shemansky's function and ours are both concave.

The origin of the difference between the earlier data and Shemansky's function is unclear. He depended only on the data of Broadfoot and Maran in the region between 1.27 and 1.43 Å, and Broadfoot and Maran's analysis used Franck–Condon factors that most likely were good ones. Nevertheless, those data and Shemansky's function are of opposite curvature.

The differences between the earlier data and our own must relate to disparate intensity measurements or data analysis. Since we have analyzed all four sets of intensity measurements with a common set of Franck–Condon factors, r centroids, and transition frequencies, the disagree-

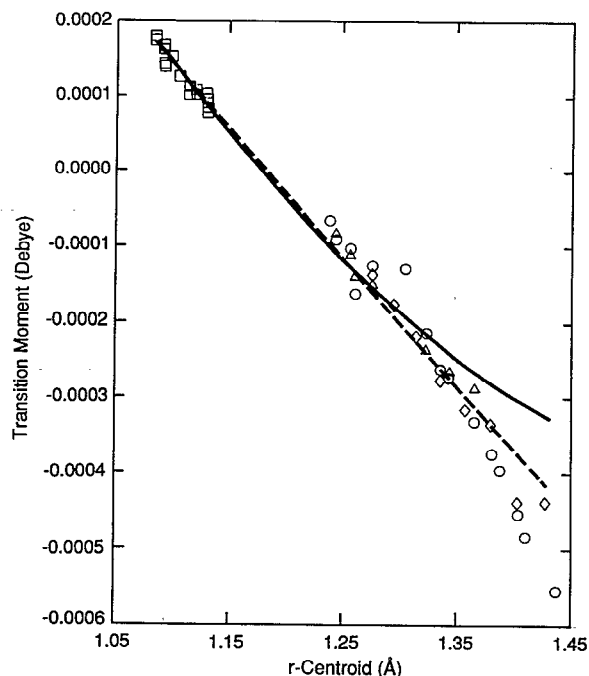


FIG. 7. A comparison of the relative transition moment data of Carleton and Papioliolis (Ref. 10) (Δ), Chandraiah and Shepherd (Ref. 11) (\circ), and Broadfoot and Maran (Ref. 12) (\diamond) with Shemansky's (Ref. 1) transition moment data (\square), his transition moment function (---), and that calculated from Eq. (6) (—). The relative data have been normalized to Shemansky's function at 1.294 Å.

ment must reside either in the intensity measurements themselves or in reducing the actual measured quantities, e.g., the current flowing out of a photomultiplier anode, to physical units, such as photons s^{-1} .

The most common source of measurement error arises in calibrating the spectroscopic measuring system for sensitivity as a function of wavelength. These calibrations involve measuring the spectrum of a lamp whose irradiance is known as a function of wavelength. Because all three of the earlier groups recorded a set of relative band intensities that were compatible with each other, we can assume that they all calibrated their spectroscopic systems with similar standards.

Our calibrations differ from those of the other groups in that our calibration standard was a deuterium lamp between 200 and 400 nm and a quartz–halogen lamp for wavelengths longer than 400 nm. The two sources agreed excellently in the region of spectral overlap 280–400 nm. The other three groups all used a tungsten strip lamp for their irradiance standard. Perhaps the root of the problem lies in these different standards. The deuterium lamp is strictly an ultraviolet standard, whereas the tungsten lamps are very faint at wavelengths shorter than about 300 or 350 nm. Thus, making accurate intensity measurements at the shortest wavelengths is particularly difficult.

A common problem arises in accounting satisfactorily for scattered light within the monochromator. Scattered light generally will lead one to overestimate calibration lamp intensities at the shorter wavelengths. Such an error

will cause band intensity measurements to be undercorrected. As a result, response corrected band intensities at short wavelengths will appear to be smaller with respect to longer wavelength band intensities than is actually the case. Such a trend is consistent with the discrepancies between the earlier data and our own.

In the present case, however, this argument is probably insufficient to rationalize the differences in the various band-intensity measurements. The discrepancies between our data and those of the other groups become most pronounced at the longer wavelengths where the standard lamp calibrations are more likely to be accurate. Another possibility might reside in augmentation of apparent band intensities by overlap with other band systems, primarily the nitrogen second-positive bands which are excited in $N_2(A)$ energy-pooling processes. Although the other groups recognized this problem and tried to apply appropriate corrections, we think our spectral fitting analysis likely accommodates overlapping emissions more accurately.

We are confident our response calibration and data analysis are correct. Using a similar approach to study the $NO(B^2\Pi - X^2\Pi)$ (Ref. 26) and $N_2(B^3\Pi_g - A^3\Sigma_u^+)$ (Ref. 8) band systems, we have determined transition moment functions that match the best available *ab initio* transition moment functions for^{8,27} these band systems to within 5%. In addition, the variation in radiative lifetime with vibrational level calculated from our transition moment functions for these two band systems follows the experimentally determined lifetime variations^{28,29} to within 5%.

B. Absolute transition moment function comparison

Figure 7 also compares our transition moment function with that proposed by Shemansky.¹ The two functions agree fairly well between 1.08 and 1.25 Å, but then begin to diverge as the internuclear distance increases further. As a result of this divergence, band intensity calculations using Einstein coefficients calculated from Shemansky's transition moment function will predict much more radiation at long wavelengths, compared to radiation levels at short wavelengths, than would be the case using Einstein coefficients calculated from our function. This difference amounts to almost a factor of 2 for transitions around 450 nm.

The difference in the shapes of the transition moment functions also results in a much steeper increase in radiative lifetime with increasing vibrational level for lifetimes calculated from our function compared to those reported by Shemansky. Table II compares radiative lifetimes calculated from the two transition moment functions. Our radiative lifetimes are larger than Shemansky's by about 25% for $v'=0$ and the discrepancy increases to almost 60% for $v'=4-6$.

C. Other considerations

Shemansky has shown that the three substates of the $N_2(A)$ state do not all have the same radiative lifetime, or equivalently, each band consists of three degenerate tran-

TABLE II. Radiative lifetimes^a of $N_2(A^3\Sigma_u^+, v)$.

Vibrational level	Present results	Shemansky ^b
0	2.37	1.91
1	2.65	1.97
2	2.88	2.02
3	3.10	2.05
4	3.24	2.08
5	3.32	2.10
6	3.31	2.13

^aUnits of seconds. These values are averaged over all spin substates.

^bReference 1.

sitions not all having the same Einstein coefficient. In most practical cases, the sublevels are in collisional equilibrium, so that each transition has only one effective radiative lifetime. Shemansky's table of Einstein coefficients gives values only for one sublevel. Our Einstein coefficients should be multiplied by a factor of 1.5 for comparison with Shemansky's values. The values in Table I are the average values for the collisionally coupled substates, and therefore need be corrected only for the unusual cases in which the differences in the behavior of the sublevels can be distinguished. Such cases require ambient pressures below about 10^{-7} Torr. For atmospheric applications, this corresponds to altitudes above about 150 km.

Studies aimed at determining product branching ratios in $N_2(A)$ energy transfer reactions generally use Vegard-Kaplan band intensity measurements to determine $N_2(A)$ number densities. Using our Einstein coefficients will result in somewhat larger $N_2(A)$ number densities than are obtained from Shemansky's Einstein coefficients. The larger $N_2(A)$ number densities will translate to smaller excitation rate coefficients or branching ratios. The magnitude of the correction depends on how the Vegard-Kaplan photometry has been accomplished.

In some cases, $N_2(A)$ number densities are determined by observing a single Vegard-Kaplan band, e.g., the 0,6 band for $v'=0$ and the 1,9 or 1,10 bands for $v'=1$. In this case, the appropriate corrections can be determined directly by comparing the Einstein coefficients in Table I with those in Table VI of Shemansky's paper,¹ being sure to apply the factor of 1.5 correction to put the two sets on a common basis.

In our work, we usually use spectral fitting techniques to determine the $N_2(A)$ number densities. The discrepancies in number densities calculated using the two different Einstein coefficient sets will then depend on the range in wavelengths over which the Vegard-Kaplan spectra have been fit. Fits over the wavelength range between 200 and 260 nm using the two different sets of transition probabilities will give $N_2(A, v'=0,1,2)$ number densities that differ from each other by less than 10%. On the other hand, fits between 400 and 500 nm will result in number densities of $N_2(A, v=0)$ 45%–50% and $N_2(A, v'=1,2,3)$ almost 60% larger using our Einstein coefficients instead of Shemansky's.

The more normal situation is for the Vegard-Kaplan spectra to begin between 220 and 250 nm and extend to

between 370 and 400 nm. In this situation, our transition probabilities will give number densities for $N_2(A, v'=0)$ 15%–20%, $N_2(A, v'=1)$ 25%–35%, and $N_2(A, v'=2)$ 40%–50% larger than those calculated from Shemansky's transition probabilities. Given a typical vibrational distribution of 1:0.6:0.2 for $v'=0,1,2$, respectively, as calculated using Shemansky's Einstein coefficients, overall $N_2(A)$ number densities will be about 25% larger if calculated using our transition probabilities. This will result in product excitation rate coefficients or branching ratios^{7,30–35} about 25% smaller than published values. In the case of $N_2(A)$ energy-pooling studies,^{15,36} where the square of the $N_2(A)$ number density is important, the rate coefficients will decrease by about 50%. If state specific product measurements have been made, then the product formation rate coefficients have to be corrected appropriately for the individual vibrational levels.

For example, the current studies were initiated because we observed a rate coefficient for exciting $NO(A)$ by $N_2(A, v'=0)$ that was about 40% greater than the total rate coefficient for $N_2(A, v'=0)$ quenching by NO .⁷ This discrepancy initially led us to suspect a problem with the Einstein coefficients of either the nitrogen first-positive or the Vegard–Kaplan systems. Our current results indicate that $N_2(A)$ number densities in our study of the excitation of $NO(A)$ by $N_2(A)$ were underestimated by about 20%. Using the Einstein coefficients in Table I to correct the earlier results makes the rate coefficient for $NO(A)$ excitation by $N_2(A)$ $(8.3 \pm 2.5) \times 10^{-11} \text{ cm}^3 \text{ molecule}^{-1} \text{ s}^{-1}$, which is more in accord with the rate coefficient for $N_2(A)$ quenching by NO $(6.6 \pm 1.0) \times 10^{-11} \text{ cm}^3 \text{ molecule}^{-1} \text{ s}^{-1}$ although still, annoyingly, 25% larger.

Those studies also indicated that $N_2(A, v'=1)$ excited $NO(A)$ 22% more rapidly than does $N_2(A, v'=0)$. Correcting these results for our Einstein coefficients results in only an 8% increased efficiency for $N_2(A, v'=1)$. This difference is smaller than the experimental uncertainty in the measurements. On the other hand, $N_2(A, v' \geq 2)$ was determined to be only 55% as efficient at exciting $NO(A)$ as $N_2(A, v'=0)$. Correcting this ratio will reduce this number to 45%.

Subsequent to the $N_2(A)/NO$ work, we and others^{31–33} noted excess product formation in several other $N_2(A)$ energy transfer systems in which the $N_2(A)$ number densities were determined by $N_2(A)$ Vegard–Kaplan emission. In most instances, correcting the previous results with our Einstein coefficients is insufficient to resolve these discrepancies. This problem appears more to result from an addi-

tional, so far unobserved metastable produced in the energy transfer reaction between $Ar^*(^3P_{2,0})$ and N_2 .

ACKNOWLEDGMENTS

We appreciate financial support from the Air Force Office of Scientific Research (Task 2310G4) and the Defence Nuclear Agency (Project SA, Task SA/SDI, work unit 00175) through a contract with the Phillips Laboratory/Geophysics Directorate F19628-88-C-013.

- ¹D. E. Shemansky, *J. Chem. Phys.* **51**, 689 (1969).
- ²D. E. Shemansky and N. P. Carleton, *J. Chem. Phys.* **51**, 682 (1969).
- ³N. P. Carleton and O. Oldenberg, *J. Chem. Phys.* **36**, 3460 (1967).
- ⁴D. E. Shemansky and A. Vallance Jones, *Planet. Space Sci.* **16**, 1115 (1968).
- ⁵W. Benesch, J. T. Vanderslice, S. G. Tilford, and P. G. Wilkinson, *Astrophys. J.* **143**, 408 (1966).
- ⁶M. Jeunehomme, *J. Chem. Phys.* **45**, 1805 (1966).
- ⁷L. G. Piper, L. M. Cowles, and W. T. Rawlins, *J. Chem. Phys.* **85**, 3369 (1986).
- ⁸H. J. Werner, J. Kalcher, and E. A. Reinsch, *J. Chem. Phys.* **81**, 2420 (1984).
- ⁹L. G. Piper, K. W. Holtzclaw, B. D. Green, and W. A. M. Blumberg, *J. Chem. Phys.* **90**, 5337 (1989).
- ¹⁰N. P. Carleton, and C. Papaliolios, *J. Quant. Spectrosc. Radiat. Transfer* **2**, 241 (1962).
- ¹¹G. Chandraiah and G. G. Shepherd, *Can. J. Phys.* **46**, 221 (1968).
- ¹²A. L. Broadfoot and S. P. Maran, *J. Chem. Phys.* **51**, 678 (1969).
- ¹³D. H. Stedman and D. W. Setser, *Chem. Phys. Lett.* **2**, 542 (1968).
- ¹⁴D. W. Setser, D. H. Stedman, and J. A. Coxon, *J. Chem. Phys.* **53**, 1004 (1970).
- ¹⁵L. G. Piper, *J. Chem. Phys.* **88**, 231 (1988).
- ¹⁶C. Effantin, C. Amiot, and J. Verges, *J. Mol. Spectrosc.* **76**, 221 (1979).
- ¹⁷F. Roux, F. Michaud, and J. Verges, *J. Mol. Spectrosc.* **97**, 253 (1983).
- ¹⁸A. Lofthus and P. Krupenie, *J. Phys. Chem. Ref. Data* **6**, 113 (1977).
- ¹⁹K. P. Huber and G. Herzberg, *Constants of Diatomic Molecules* (Van Nostrand Reinhold, New York, 1977).
- ²⁰L. G. Piper and L. M. Cowles, *J. Chem. Phys.* **85**, 2419 (1986).
- ²¹W. J. Marinelli and L. G. Piper, *J. Quant. Spectrosc. Radiat. Transfer* **34**, 121 (1985).
- ²²P. A. Fraser, *Can. J. Phys.* **32**, 515 (1954).
- ²³R. W. Nicholls, *J. Quant. Spectrosc. Radiat. Transfer* **14**, 233 (1974).
- ²⁴J. C. McCallum, *J. Quant. Spectrosc. Radiat. Transfer* **21**, 563 (1979).
- ²⁵D. L. Albritton, A. L. Schmeltekopf, and R. N. Zare (unpublished, 1971).
- ²⁶L. G. Piper, T. R. Tucker, and W. P. Cummings, *J. Chem. Phys.* **94**, 7667 (1991).
- ²⁷S. R. Langhoff, H. Partridge, R. W. Bauschlicher, and A. Komornicki, *J. Chem. Phys.* **94**, 6638 (1991).
- ²⁸G. E. Gadd and T. G. Slanger, *J. Chem. Phys.* **92**, 2194 (1990).
- ²⁹E. E. Eyler and F. M. Pipkin, *J. Chem. Phys.* **79**, 3654 (1983).
- ³⁰M. E. Fraser and L. G. Piper, *J. Phys. Chem.* **93**, 1107 (1989).
- ³¹L. G. Piper, *J. Chem. Phys.* **90**, 7087 (1989).
- ³²T. D. Dreiling and D. W. Setser, *Chem. Phys. Lett.* **74**, 211 (1980).
- ³³L. G. Piper, W. J. Marinelli, W. T. Rawlins, and B. D. Green, *J. Chem. Phys.* **83**, 5602 (1985).
- ³⁴L. G. Piper, *J. Chem. Phys.* **77**, 2373 (1982).
- ³⁵L. G. Piper, *J. Chem. Phys.* **91**, 864 (1989).
- ³⁶L. G. Piper, *J. Chem. Phys.* **88**, 6911 (1988).